

TWO-PARTICLE CORRELATION AND JET
MEASUREMENTS IN e^+e^- COLLISIONS AT 91 GeV
WITH ARCHIVED ALEPH DATA*

YI CHEN, MICHAEL JOSEPH PETERS, TZU-AN SHENG, YEN-JIE LEE
YU-CHEN CHEN

Massachusetts Institute of Technology, USA

ANTHONY BADEA

Harvard University, USA

AUSTIN ALAN BATY

Rice University, USA

CHRISTOPHER MCGINN, DENNIS PEREPELTSIA

Colorado University Boulder, USA

GIAN MICHELE INNOCENTI

CERN, Switzerland

MARCELLO MAGGI

Istituto Nazionale di Fisica Nucleare Sezione di Bari, Italy

PAOTI CHANG

National Taiwan University, Taiwan

*Received 11 September 2022, accepted 10 October 2022,
published online 14 December 2022*

The first measurement of anti- k_T jets and two-particle angular correlations of charged particles emitted in high energy e^+e^- annihilation is presented. The archived data at a center-of-mass energy of 91 GeV were collected with the ALEPH detector at LEP between 1992 and 1994. At 91 GeV, no significant long-range correlation was observed in either the laboratory coordinate analysis or the thrust coordinate analysis, where the

* Presented at the 29th International Conference on Ultrarelativistic Nucleus–Nucleus Collisions: Quark Matter 2022, Kraków, Poland, 4–10 April, 2022.

latter is sensitive to a medium expanding transverse to the color string between the outgoing $q\bar{q}$ pair from Z boson decays. We also present the first measurement of anti- k_T jet energy spectra and substructures compared to various event generators, NLO, and NLL^1+R resummation calculations.

DOI:10.5506/APhysPolBSupp.16.1-A71

1. Introduction

Hadronic colliders have observed quark–gluon plasma-like signatures in progressively smaller systems. One of the examples is the long-range correlation particles. A ridge-like structure has been observed in high multiplicity proton–proton (pp) collisions [1]. In nucleus–nucleus collisions, the long-range structure is interpreted as the consequence of an expanding quark–gluon plasma, while for smaller collision systems, the interpretation is less clear. In order to gain more insight into the origin of such a correlation in small systems, it is, therefore, interesting to search for it in e^+e^- collisions, where there is no complication of hadronic initial state. Jet measurements are also of interest in e^+e^- collisions. Jet measurements in LEP (see *e.g.* [2]) were limited to earlier generation of jet-finding algorithms and, therefore, not directly comparable to more recent measurements (*e.g.* [3–6]) from the hadron colliders, where the anti- k_T algorithm [7] is commonly used. In this work, we reanalyze the ALEPH e^+e^- collision data taken during LEP1 at 91.2 GeV to search for potential ridge-like structure in two-particle correlations [8]. A first measurement of the jet energy spectra and substructure with the anti- k_T algorithm is also reported [9].

2. Two-particle correlation

The two-particle correlation results are investigated in two different coordinate systems: laboratory coordinate and thrust [10] coordinate. In the laboratory coordinate analysis, the reference axis is the laboratory direction defined by the incoming e^+ and e^- beams. This coordinate system is the most similar to what is done in hadronic colliders, where the result is sensitive to a potential quark–gluon plasma expanding perpendicular to the incoming beams. The second coordinate system is defined with respect to the thrust axis, or the direction of the dominant outgoing energy flow. In the case of a dijet event, the thrust axis will be aligned with the back-to-back dijet. The results will be sensitive to a potential quark–gluon plasma expanding perpendicular to the dijet system.

Pairs of charged particles are paired from each event to form the raw two-particle correlation function. They are then corrected by the “background” correlation function to account for acceptance effects. They are constructed

using particles paired from different events to eliminate all physics-induced correlations. The corrected correlation function is then examined and the ridge-like effect is searched for in the large $|\Delta\eta|$ region. The correlation function is projected in the $|\Delta\phi|$ variable with a selection of $1.6 < |\Delta\eta| < 3.2$ to reduce correlation from particle pairs from the dominant back-to-back dijet topologies. The function is then shifted following the ZYAM scheme [11] before quantifying potential yield from the ridge-like signature. The procedure is repeated with events in different N_{trk} ranges, inspired by the results in pp collisions at the LHC, where ridge-like signature is only observed in high multiplicity events.

An example of the projected correlation function is shown in Fig. 1 for the laboratory coordinate system in the left panel and the thrust coordinate system in the right panel. In both cases, we observe a relatively stronger back-to-back correlation with $|\Delta\phi| \sim \pi$ compared to the near side. The function, however, does not show any signs of a potential ridge signal, which will manifest itself as an enhancement at $|\Delta\phi| \sim 0$.

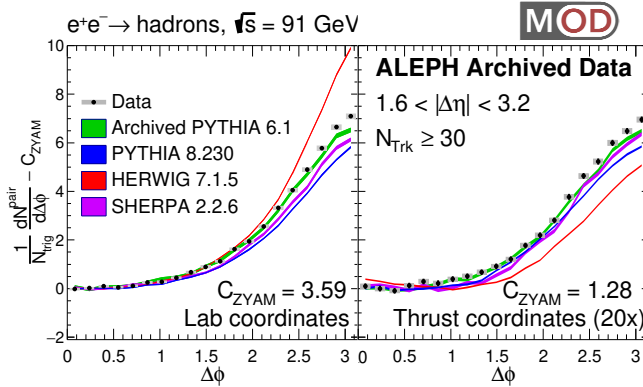


Fig. 1. Correlated yield obtained from the ZYAM procedure as a function of $|\Delta\phi|$ averaged over $1.6 < |\Delta\eta| < 3.2$ in laboratory (left) and thrust (right) coordinate analyses.

In the absence of any observed ridge-like effects, limits on potential near-side yield enhancement are extracted, shown in Fig. 2 for both results from the laboratory coordinate and the beam coordinate systems. The limits are also compared with proportionately-scaled results from the CMS experiment on hadronic collision systems. The extracted limits are compatible with or lower than the corresponding results from the CMS experiment, however the uncertainty is large and prevents a quantitative statement for this dataset.

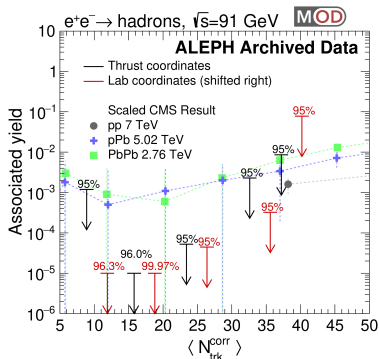


Fig. 2. (Color online) Limits on the associated yield as a function of corrected number of tracks. The results from laboratory (thrust) coordinates are shown as red (black) arrows. The laboratory data have been shifted right three units for clarity.

3. Jet measurements

In the current work [9], inclusive jet energy spectrum, leading dijet energy spectrum, leading dijet total energy, and inclusive jet substructure (jet mass normalized by jet energy M/E , groomed jet mass normalized by energy M_G/E , groomed jet momentum sharing z_G and angle R_G) are measured.

Jets are clustered [12] from the energy flow objects with the e^+e^- version of the anti- k_T algorithm [7] using energy instead of k_T and opening angle instead of $\Delta R \equiv \sqrt{\Delta\eta^2 + \Delta\phi^2}$. The jet resolution parameter R is chosen to be 0.4 in this set of results in order to compare with analogous results from the hadron colliders. Once the jets are reconstructed, dedicated calibrations are derived and applied. The energy scale of the jets is first calibrated in simulated events using the archived PYTHIA 6 simulation. Additional residual calibrations are derived for data to account for data-simulation differences based on differences between two sides of the detector and the event-wide multijet mass. The size of the residual corrections goes up to 1%. The relative difference of jet energy resolution between data and simulation is found to be up to 5%. For the jet substructure, the SoftDrop [13, 14] algorithm is used, with the setting $z_{\text{cut}} = 0.1, \beta = 0.0$.

The spectra are unfolded for detector effects. Due to jet energy smearing effects, jet substructure measurements are done in bins of jet energy with a two-dimensional unfolding. Sources of systematic uncertainties include the jet energy scale and resolution, contribution from combinatorial jets not associated with a parton from the hard process, unfolding procedure and regularization, and modeling uncertainty. For the energy spectra measurements, the dominant source is the jet energy scale and resolution, while for the substructure measurements the dominant is from modeling.

The energy spectrum from e^+e^- collisions at 91.2 GeV is shown in Fig. 3. In the left panel, the spectrum is compared with PYTHIA 6, PYTHIA 8, Herwig 7.2.2, and Sherpa generators. None of the popular event generators reproduce the spectrum fully. The deviation at lower jet energy points to potential room for improvement in wide-angle energy and multijet production. The result is also compared with NLO parton level spectrum and NLL' R -resummed calculation [15].

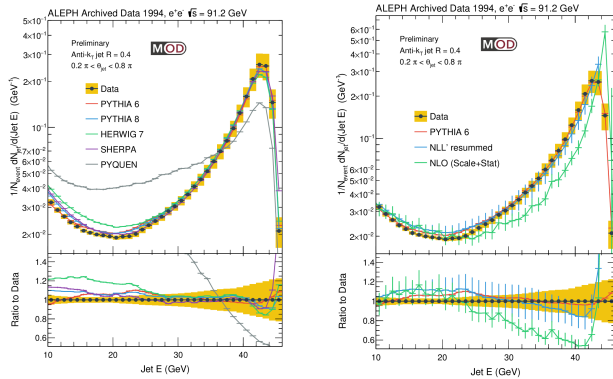


Fig. 3. Measured inclusive jet energy spectrum, normalized by the number of events used to perform the measurement. Left: The data are compared with predictions from various generators, normalized to have the same area as the data. Right: The data spectra are compared with pQCD calculations.

An example of the jet substructure result is shown in Fig. 4. The left panel shows the invariant mass of the sum of all constituents of the jet, while the right panel shows the mass of the groomed jet. They are also compared

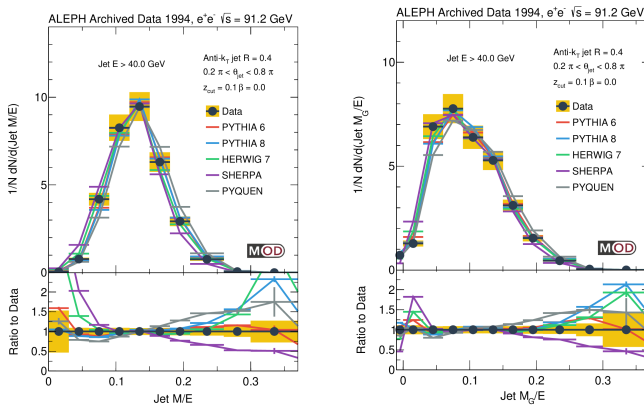


Fig. 4. Measured jet mass (left) and groomed jet mass (right) for inclusive jets. The data are compared with predictions from various generators.

with the same event generators. All the generators capture the bulk well, however, there is some deviation toward the tails. We direct the reader to our recent paper [9] for the complete set of results.

4. Summary and outlook

Measurements on two-particle correlations and anti- k_T jet are reported using the archived ALEPH e^+e^- collision data at 91.2 GeV. In contrast to results from hadronic collisions systems, the potential ridge-like signature is not observed in the correlation function and the limits are reported. These results provide new insights into the nature of the long-range correlations in smaller systems. The first measurement of the anti- k_T jet in e^+e^- collisions can provide input to theory calculation and tuning of event generators.

With the LEP2 data at higher energy, the kinematic reach of the measurements is expected to be higher, and it will be interesting to follow up with additional studies. The calibrated jets are also an excellent testing ground for the new algorithm developed for other collision systems, and they can be used to provide clean alternative measurements without the complication of hadronic initial states, providing additional insights not easily obtained from only hadronic collision systems.

REFERENCES

- [1] CMS Collaboration (V. Khachatryan *et al.*), *J. High Energy Phys.* **2010**, 91 (2010).
- [2] ALEPH Collaboration (D. Buskulic *et al.*), *Phys. Lett.* **B384**, 353 (1996).
- [3] A. Abdesselam *et al.*, *Eur. Phys. J. C* **71**, 1661 (2011).
- [4] G.P. Salam, *Eur. Phys. J. C* **67**, 637 (2010).
- [5] A. Altheimer *et al.*, *J. Phys. G: Nucl. Part. Phys.* **39**, 063001 (2012).
- [6] A.J. Larkoski, I. Moulton, B. Nachman, *Phys. Rep.* **841**, 1 (2020).
- [7] M. Cacciari, G.P. Salam, G. Soyez, *J. High Energy Phys.* **2008**, 04 (2008).
- [8] A. Badae *et al.*, *Phys. Rev. Lett.* **123**, 2002 (2019).
- [9] Y. Chen *et al.*, *J. High Energy Phys.* **2022**, 8 (2022).
- [10] E. Farhi, *Phys. Rev. Lett.* **39**, 1587 (1977).
- [11] T.A. Trainor, *Phys. Rev. C* **81**, 014905 (2010).
- [12] M. Cacciari, G.P. Salam, G. Soyez, *Eur. Phys. J. C* **72**, 1896 (2012).
- [13] A.J. Larkoski, S. Marzani, G. Soyez, J. Thaler, *J. High Energy Phys.* **2014**, 146 (2014).
- [14] M. Dasgupta, A. Fregoso, S. Marzani, G.P. Salam, *J. High Energy Phys.* **2013**, 29 (2013).
- [15] D. Neill, F. Ringer, N. Sato, *J. High Energy Phys.* **2021**, 41 (2021).